Remote Sensing of Environment 211 (2018) 1–12

Contents lists available at ScienceDirect

Remote Sensing of Environment

journal homepage: www.elsevier.com/locate/rse

The accuracy of snow melt-off day derived from optical and microwave radiometer data — A study for Europe

Sari Metsämäki[a,*], Kristin Böttcher[a], Jouni Pulliainen[b], Kari Luojus[b], Juval Cohen[b], Matias Takala[b], Olli-Pekka Mattila[a], Gabriele Schwaizer[c], Chris Derksen[d], Sampsa Koponen[a]

[a] Finnish Environment Institute, Finland
[b] Finnish Meteorological Institute, Finland
[c] ENVEO IT GmbH, Austria
[d] Environment Canada, Canada

ARTICLE INFO

Keywords:
Snow
Fractional snow cover
FSC
Melt-off day
Microwave radiometer data
Optical data
Snow water equivalent

ABSTRACT

This paper describes the methodology for deriving yearly pixel-wise snow melt-off day maps from optical data-based FSC (Fractional Snow Cover) without conducting any interpolation for cloud-obscured pixels or otherwise missing data. The Copernicus CryoLand Pan-European FSC time series for 2001–2016 re-gridded to 0.1° serves as input for the production of 16 years of melt-off day maps for Europe. These maps are compared with passive microwave radiometer (MWR) melt retrievals, to compare the performance of these two independent datasets, particularly concerning the effect of physiographic and snow conditions on the accuracy of the melt-off day estimates. Both these datasets are evaluated against melt-off day derived from in situ snow depth (SD) time series observed at European weather stations. We also present the relationship of these snow melt-off day products to a passive microwave radiometer-derived landscape freeze/thaw product.

Our results show that the melt-off day derived from optical springtime FSC time series provides the strongest correlation with the snow melt-off day with respect to the in situ data. Overall the deviation of CryoLand FSC data derived melt-off day to that indicated by in situ observations is quite small, with positive bias of 0.9 days, and RMSE of 13.1 days. For 85% of the analyzed cases the differences are between ± 10 days. Across Europe the MWR-based detection of melt-off day is less accurate; the investigated method performs the best for areas with sustained seasonal snow cover. Based on the time series for MWR-based melt-off day (1980–2016) and FT-ESDR (1980–2014), separately for boreal forests and tundra, we also found a clear trend towards earlier snow clearance: a decrease of melt-off day by as much as ~5 days per decade in boreal forest region was observed.

1. Introduction

The mid- and high-latitude areas of Europe are characterized by seasonal snow cover. Snow cover melt influences freshwater runoff, nutrient cycles and animal and plant phenology and productivity (Vaganov et al. 1999; Aurela et al. 2004; Grippa et al. 2005; Cooper et al. 2011). In addition, snow melt timing can serve as a predictor for the onset of photosynthetic (Thum et al. 2009; Böttcher et al. 2014) and animal activity (Pöyry et al. 2017) in boreal areas. Snow cover has a strong impact on the surface albedo; therefore timing of both the melt onset and the final melt-off (snow disappearance) are of great interest. Surface albedo determines the energy budget at the surface, and one of the most immediate and dynamic modifications to surface albedo is snow cover (Barlage et al. 2005). The response of snow albedo to temperature changes over seasonally snow-covered areas is described as the snow albedo feedback. This essential mechanism is a topic of many observational and climate modelling studies (e.g. Thackeray et al. 2014; Qu and Hall 2007) for which observational estimates of snow cover are required.

Statistics of European snow cover duration, snow onset and melt-off dates have been derived from MODIS snow products by Dietz et al. (2012). We investigate the snow melt-off dates for years 2001–2016 using two different Earth observation-based snow products: i) Pan-European Fractional Snow Cover (FSC) product based on the *SCAmod* method described in Metsämäki et al. (2005, 2012), provided through the Copernicus CryoLand service funded by the European Commission (Nagler et al., 2015), and ii) Melt-off day product derived from passive microwave data produced by an algorithm developed at the Finnish Meteorological Institute (Takala et al. 2009). The latter served as input also for Snow Water Equivalent (SWE) products as provided within ESA

* Corresponding author.
E-mail address: sari.metsamaki@ymparisto.fi (S. Metsämäki).

https://doi.org/10.1016/j.rse.2018.03.029
Received 12 May 2017; Received in revised form 16 March 2018; Accepted 19 March 2018

DUE GlobSnow project (Takala et al. 2011). Additionally, the Freeze/Thaw Earth System Data Record (FT-ESDR) (Kim et al. 2011, 2014) which provides estimates of landscape freeze/thaw state is compared to the passive microwave melt-off day product. The goal of the investigation is to assess the accuracy of the above listed melt-off day products as well as the possible differences between them. The applied products used in our study are all fully independent.

There are different definitions for melt-off day: it may be interpreted as the first day with snow water equivalent (SWE) = 0 mm after winter seasons' maximum SWE or, alternatively, the first day with SWE = 0 mm with no subsequent snow until new snow accumulation season takes place in the following autumn. The latter condition may be met substantially later than the former, since short periods of snow cover may occur after the primary melt event (Räisänen et al. 2014). In this paper we use the latter definition, with the exception that less than three days duration late season snow periods are allowed without an effect on the identified melt-off. There are also other terms for melt-off day found in the literature, see e.g. Lindsay et al. (2015) who use LSD (Last Snow Day), related to Melt-off Day (MoD) as MoD = LSD + 1; and Dietz et al. (2012) who use SCM (Snow Cover Melt). In this paper we use a notation MoD for Melt-off Day (snow clearance), indicating the first day of snow-free period after seasonal snow period.

We are interested in the spring time snow depletion as according to e.g. Déry and Brown (2007) and Derksen and Brown (2012), springtime trends are more evident and have the greatest potential to affect the surface radiation budget, compared to weaker trends in snow cover in fall.

2. Data sets

This section describes the datasets used in this study. Table 1 shows a summary with more detailed descriptions for each dataset in the following sub-sections.

2.1. CryoLand fractional snow cover products

The CryoLand Pan-European snow cover service (Nagler et al. 2015), currently available under the umbrella of the Copernicus Global Land service — Cryosphere theme), provides a homogeneous set of fractional snow cover products from November 2000 till present for the area extending from 72°N/11°W to 35°N/45°E with a spatial resolution of 0.005° × 0.005°. The product uses NASA Terra/MODIS (Moderate Imaging Spectroradiometer) data as input. Since February 2016, the cloud screening is based on a simple cloud detection algorithm *SCDA*, (Metsämäki et al., 2015). Prior to this, the cloud mask product of Terra/MODIS (Ackerman et al., 2010) was used. The sub-pixel FSC retrieval relies on the *SCAmod* method (Metsämäki et al. 2005, 2012), which is designed to perform well particularly in forest areas by utilizing a predetermined forest transmissivity map and a reflectance model. The transmissivity map, available for Europe and the Northern Hemisphere quantifies the transparency of the forest canopy at a pixel level and is related to crown coverage (see further details in Metsämäki et al., 2015). Since SCAmod is very sensitive to the reflectance fluctuations at the reflectance values close to those of a snow-free ground, an additional snow test is applied to the at-satellite brightness temperature as provided by the thermal infrared band 32 (*BT12*, centered at 12 μm) and on the Normalized Difference Snow Index NDSI (= [Band4 − Band6] / [Band4 + Band6]; Hall and Riggs, 1995) to discriminate between snow-free and snow cases. For the FSC production (see example in Fig. 1), only those observations that pass the snow test (BT12 < 283 K and NDSI > threshold (which is latitude, elevation and surface class dependent; Schwaizer et al. 2017) are ingested by SCAmod.

2.2. Melt-off day based on Takala et al. (2009) algorithm

The algorithm to map snow melt in Eurasia by Takala et al. (2009) is based on time series of channel differences of frequencies 18/19 GHz and 36/37 GHz, measured by several microwave radiometers. Takala et al. (2009) produced a time series of snow melt-off in Eurasia for years 1979–2007, validated using point-wise ground truth data from the extensive quality controlled INTAS-SCCONE (International Association for the promotion of co-operation with scientists from the New Independent States of the former Soviet Union — Snow Cover Changes Over Northern Eurasia set derived from weather station observations; Kitaev et al. 2002). Comparison of melt-off days with INTASS SCCONE observations showed a bias of 0.6 days for Scanning Multi-channel Microwave Radiometer (SMMR) and bias of 1.1 days for Special Sensor Microwave/imager (SSM/I), and RMSE of 22.5 and 22.2 days respectively (Takala et al. 2009). This indicates that the passive microwave melt retrievals generally correspond well with the ground-observed values of SCD over continental Eurasia. Moreover, as the algorithm is based on the pixel-wise time series analysis of space-borne observed difference between brightness temperatures observed at 37 GHz and 19 GHz vertically polarized channels (T37v–T19v), it compensates for the disturbing effect of spatially varying vegetation (forest) cover. In particular, the flag for snow status was used in the comparison. The snow melt reference value was obtained by identifying the day when the flag changed from the value “snow depth is correct” to either “temporary melting” or to “continuous melting”. If there were more than one such change only the last one was taken into account. In addition, Takala et al. (2009) compared the results to optically derived SCA (Snow Covered Area) data to show that, in case of boreal regions, point-wise observations on snow conditions can provide information concerning larger landscapes (spatial resolution of about 25 km) in validation processes. The dataset applied here is further extended to

Table 1
Datasets used in the study.

Abbreviation	FSC	MoD_{Opt}	MoD_{MWR}	$TD_{FT\text{-}ESDR}$
EO data source	Terra/MODIS	Terra/MODIS	SMMR, SSM/I, SSM/S, AMSR-E	SMMR,SSM/I, SSM/S, AMSR-E
Product	CryoLand Fractional Snow Cover (FSC)	Melt-off day for Europe based on CryoLand FSC	Snow melt-off day for Eurasia	daily Landscape Freeze/Thaw status
Time period	2001–2016	2001–2016	1980–2016	1980–2014
Information	Fractional Snow Cover (% of the grid cell area)	Snow melt-off day	Snow melt-off day	Landscape Freeze-to-thaw day
Original coordinate grid of the product	0.005° WGS-84	0.005° WGS-84	25 km EASE-Grid	25 km EASE-Grid
Resolution used in the study	0.1° WGS-84 (re-gridded)	0.1° WGS-84 (re-gridded)	0.1° WGS-84 (re-gridded); 25 km EASE-Grid	0.1° WGS-84 (re-gridded); 25 km EASE-Grid
Reference to the product/ algorithm	Nagler et al. 2015; Schwaizer et al. 2017; Metsämäki et al. 2005, 2012	Nagler et al. 2015; Schwaizer et al. 2017; Metsämäki et al. 2005, 2012	Takala et al. 2009	Kim et al. 2011, 2014

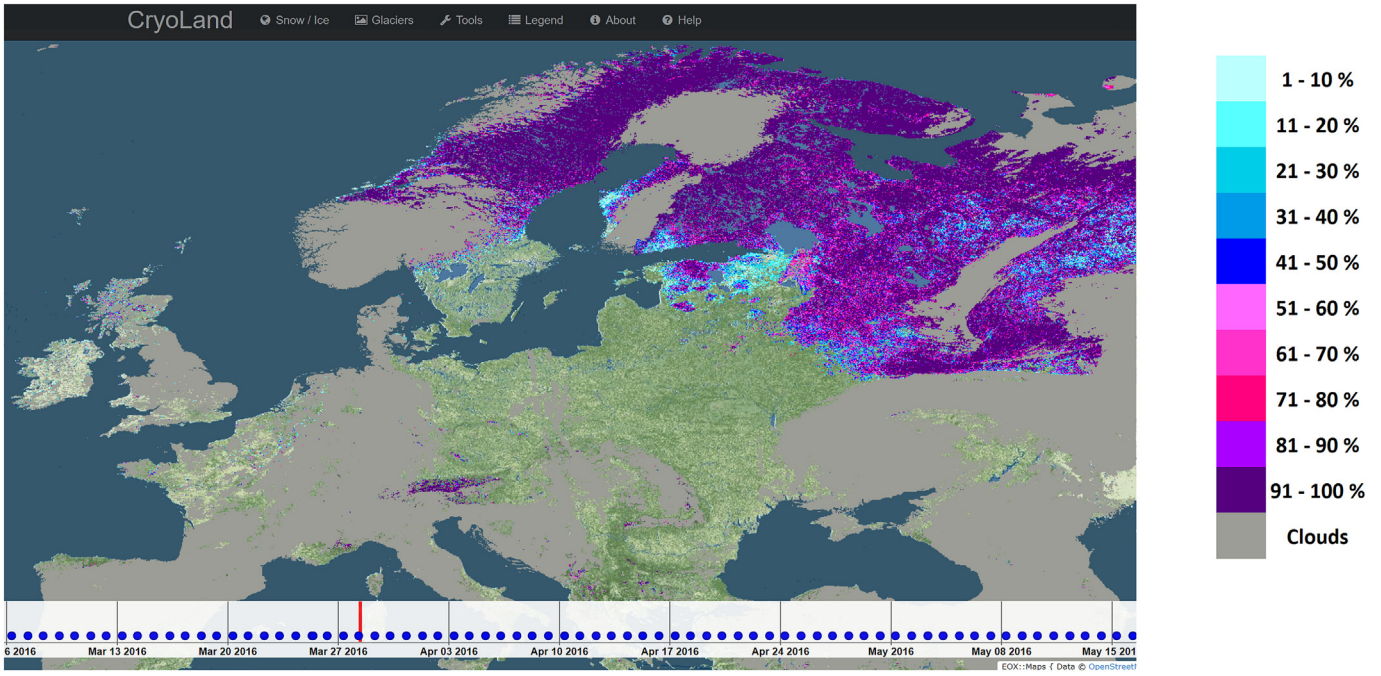

Fig. 1. CryoLand Pan-European Fractional Snow Cover (FSC) product on the 28th March 2016. Grey color indicates clouds; dark green/blue indicates water. (For interpretation of the references to color in this figure legend, the reader is referred to the web version of this article.)

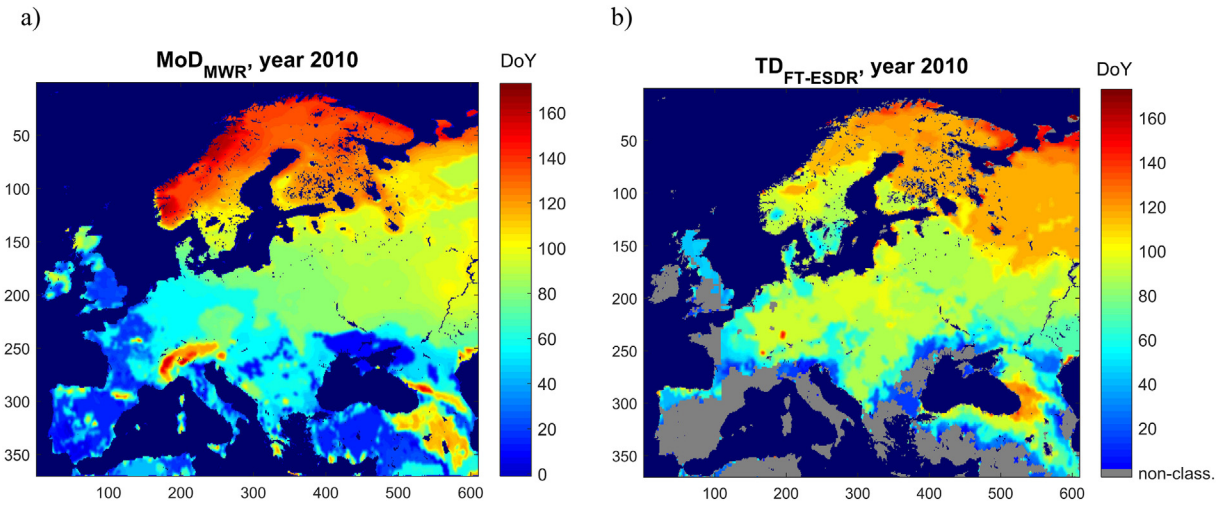

Fig. 2. Snow melt-off day in 0.1° grid for 2010: a) MoD_{MWR} and b) $TD_{FT\text{-}ESDR}$. Melt-off day is given as Day of Year, i.e. starting from January the 1st. Dark blue areas represent water. (For interpretation of the references to color in this figure legend, the reader is referred to the web version of this article.)

include all spring melt periods in 1980–2016. Water bodies are masked out of the product; the water mask is based on the Global Land Cover Map (GLC2000; Bartholome and Belward, 2005). The GLC2000 classification was first mapped to EASE Grid (corresponding to radiometer data) and then the fraction of water bodies within each grid cell was calculated. If this fraction exceeds 50%, a cell is classified as "Water". An example of MWR-based melt-off day map for 2010 (denoted as MoD_{MWR} in this paper) is given in Fig. 2a). The original melt-off day data was re-gridded to 0.1° to make it easy to compare with optical data-based melt-off day. Cubic-spline interpolation was chosen for the re-gridding as it results in a smooth surface in the northern latitudes where the original EASE-Grid cells contain only a few 0.1° target cells. Nearest neighbor or bilinear interpolation would have resulted in a surface with arbitrary discontinuities. The same interpolation approach was also applied to the re-gridded FT-ESDR dataset used in this study.

2.3. Freeze/thaw information from passive microwave radiometer data

The Freeze/Thaw Earth System Data Record (FT-ESDR) described in Kim et al. (2011, 2014) provides estimates of landscape thaw based on spaceborne passive microwave radiometer observations. The landscape thaw mapping is performed using a change detection algorithm that has grid cell-by-cell thresholds dynamically optimized with global near-surface air temperature from reanalysis data. The FT-ESDR algorithm optimization identifies (by linear regression) the moment when the value of the microwave radiometer derived index corresponds to the zero crossing of air temperature. In this study, the thaw date (denoted here as $TD_{FT\text{-}ESDR}$) was derived from the primary thaw date, when the landscape undergoes a persistent thaw transition to predominantly non-frozen conditions in the spring. The primary thaw date is derived using both FT-ESDR classified daily non-frozen and transitional (AM frozen, PM thaw) conditions. Thus, $TD_{FT\text{-}ESDR}$ is not a direct snow-related

retrieval, but can still be used for the comparison with the other dataset used in our study. An example for year 2010 is presented in Fig. 2b) along with the corresponding MoD_{MWR} result. The disagreement between these two products is clear, showing an earlier snow melt by MoD_{MWR} in central Europe, while in Northern Europe $MoD_{FT\text{-}ESDR}$ indicates earlier melting than MoD_{MWR}. These products and their related analyses are discussed in more detail in Section 4.2.

2.4. In situ data

In situ reference data consists of four datasets providing daily observations of snow depth: 1) Observations from the national weather station network of the Finnish Meteorological Institute (FMI); 2) Observations from the network of weather stations of the All-Russian Research Institute for Hydrometeorological Information — World Data Centre (RIHMI-WDC) and from 14 neighboring states (Bulygina et al., 2015; maintained by RIHMI-WDC); and 3) Observations from the international weather station network of the European Centre for Medium-Range Weather Forecasts (ECMWF). The ECMWF weather station network is a collection of selected stations from national weather station networks and therefore there is some overlap with the FMI and RIHMI-WDC datasets. The full dataset consists of over 1500 sites. Fig. 3 presents the in situ (weather station) locations. Boreal forest and Tundra stations from the ECMWF network are used for i) evaluation of landscape freeze/thaw retrievals in the FT-ESDR and melt-off day by Takala et al. (2009) in their original 25 km EASE-Grid system and ii) comparison of the validation results for these specific sites with the validation results obtained for MoD_{MWR}, $TD_{FT\text{-}ESDR}$, and CryoLand FSC-based MoD (all re-gridded to 0.1°), for all in-situ sites comprising ECMWF, RIHMI and FMI stations over Europe. Examples of snow depth data are shown later in Fig. 7 in Section 4 Results and discussion.

The identification of boreal forest and tundra are determined from the ESA GlobCover 2009 dataset (Bontemps et al., 2009). Since the spatial resolution of applied space-borne microwave radiometer data is in the order of 25 km, the forests and tundra regions are considered by the following criteria. A grid cell of 625 km^2 is assigned to represent boreal forest if the areal fraction of GlobCover class 90 (open conifer forests) is higher than 30%. For alpine tundra the fraction of class 150 (sparse vegetation) must be higher than 45%, and additionally, grid cells representing mountain areas with a high topographic variability (standard deviation of elevation variability > 200 within 25 km × 25 km grid cell) are masked. This masking concerns only boreal forest and tundra stations; the other in situ locations which indeed are used for analyzing 0.1° data, comprise also mountains (e.g. the Alps).

3. Methodology

3.1. Melt-off day from in situ snow depth data

In this study, melt-off day is considered as the first day of the snow-free period following at least two weeks (14 days) of snow cover defines as the Continuous Snow Season (CSS). CSS was earlier defined by Choi et al. (2010) and Lindsay et al. (2015). The latter study permitted CSS to take place at any time during the snow season, while the former paper applied temporal constraints to CSS. We allow intervening snow-free days during the snow season in general, but the melt-off day is defined only for in situ stations which provide the CSS. This practice excludes the in situ stations which report temporally very sparse snow observations. A station is considered snow-free if the observed snow depth is 0 cm. After the initial MoD is identified, a search considering also short snow-free periods (longer than 3 days after the CSS) is conducted. If such a snow period is found, the MoD is identified as the first snow-free day after this shorter period. Stations with too many data gaps or the length of the time series is < 50 days are discarded. Fig. 4 provides the description of the procedure. The in situ SD-based melt-off day is denoted as MoD_{insitu}.

3.2. Melt-off day from CryoLand FSC time series

The melt-off day from the FSC time series is identified as a beginning of a snow-free period (FSC = 0%) after a period of snow

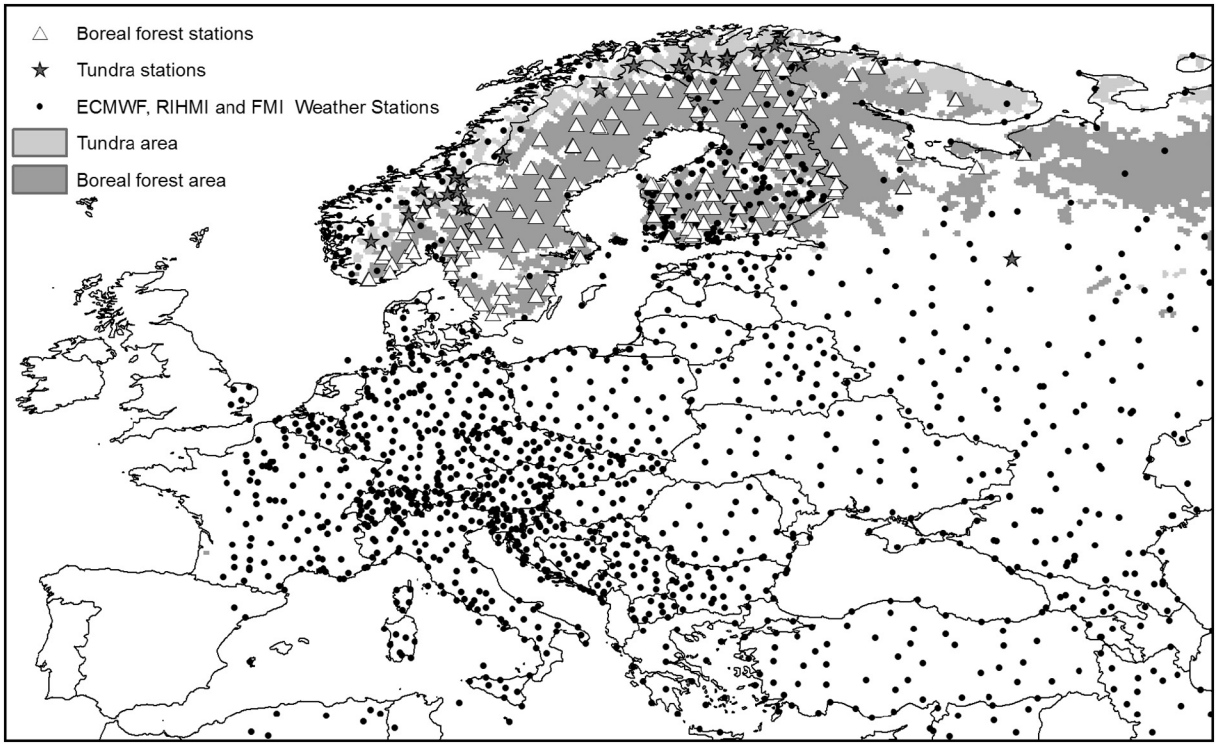

Fig. 3. In situ stations used in the investigations.

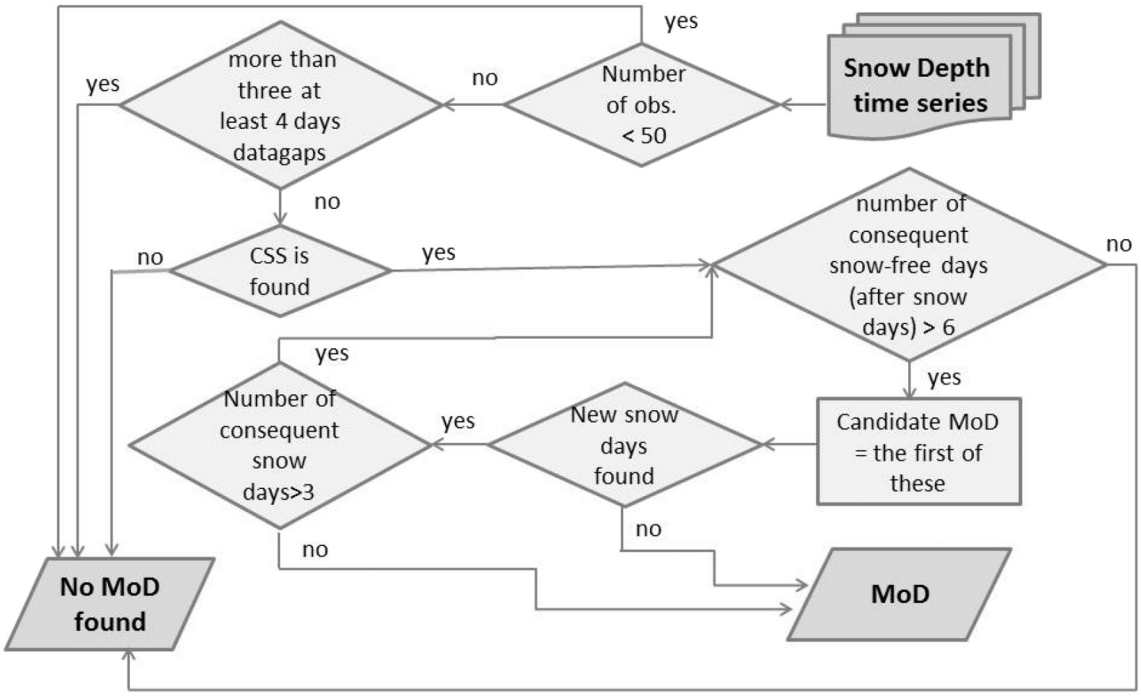

Fig. 4. Procedure for finding Melt-off Day (MoD) from in situ snow depth time series.

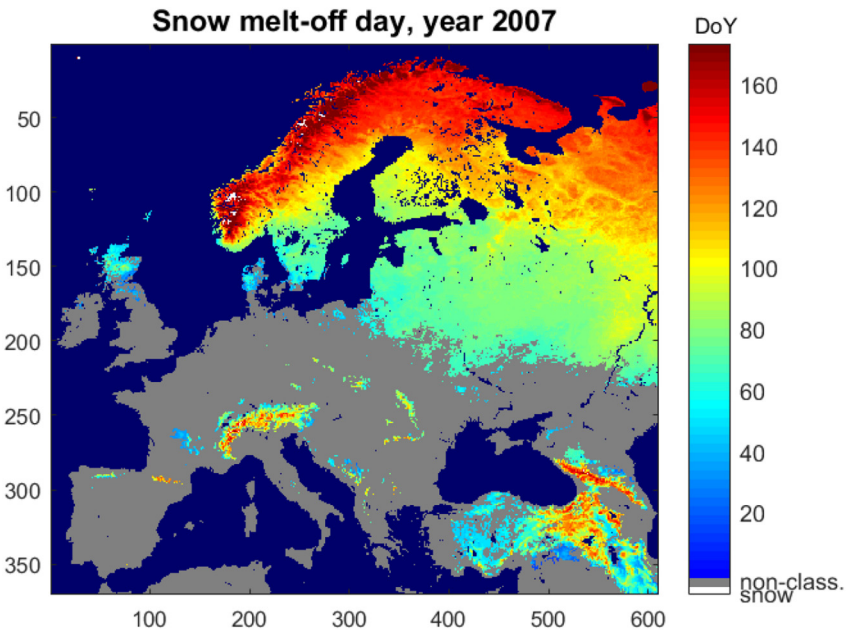

Fig. 5. Snow melt-off map (MoD_{Opt}) for 2007. Day is given as Day of Year, i.e. starting from 1st January in each year. Grey color indicates areas for which the melt-off day was not possible to determine (intermittent snow or no snow days at all), Dark blue stands for water, white stands for permanent snow. (For interpretation of the references to color in this figure legend, the reader is referred to the web version of this article.)

observations (FSC > 0%). No temporal or spatial filtering is carried out, which means that cloudy or missing observations (e.g. due to the polar darkness) makes the detection procedure challenging. We rely on non-filtered data in order to investigate the potential of the remotely sensed data as it is, without interference of any filtering and interpolation techniques which may vary (e.g. Dietz et al. 2012; Choi et al. 2010). Our procedure allows temporally sparse snow-free observations within the snow period, whilst the snow-free period can include sporadic snow observations. This is necessary to allow, as the failure of cloud screening easily produces false snow commissions whereas undetected cloud shadows may produce false snow omissions. The procedure goes as follows:

1. A pixel is assigned the status “melted” after a period of at least six subsequent snow-free days is found (however with possible intervening cloudy observations), if the number of the snow-free days represents 80% of all cloud-free observations after the first day of the snow-free period in concern. The first day of this period is accepted as a candidate for the melt-off day.
2. After a pixel is assigned the status “melted”, it is still possible to identify a new snow season if certain conditions are met. The requirements of changing the status to “new snow period” is that at least three subsequent snow days are observed so that the number of these days is larger than 2/3 of all clear-sky observations after the first day of this new snow period. If a new snow period is initiated, a new search for melt-off day is launched, and the process is repeated starting from Step 1.

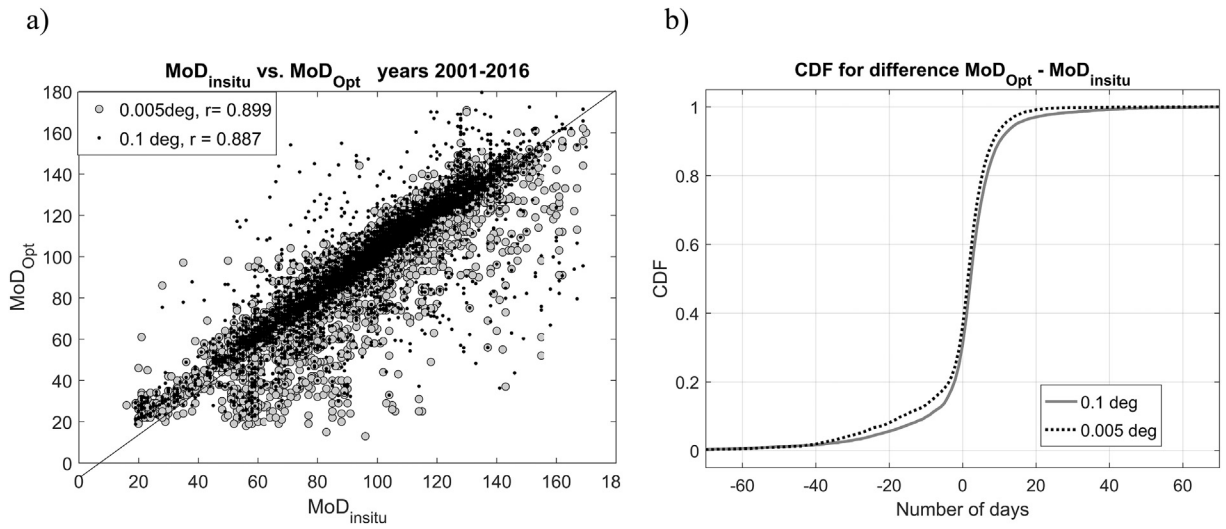

Fig. 6. a) MoD_{insitu} vs. MoD_{opt} in both resolutions with correlation coefficients, b) Cumulative Distribution Function for absolute differences ($MoD_{Opt} - MoD_{insitu}$) in both resolutions.

The extraction of melt-off day from CryoLand FSC estimates starts from 1st January; hence the snow periods taking place before that are not identified. During the winter period starting from 1st January, the intermittent snow periods can be captured when they occur during clear-sky days. Since the detection method is designed for seasonal snow, we discard the cases where snow days are temporally very sparse. This is justified as there is not a well-defined melt-off day for locations for which only sporadic snow fall and rapid melting are typical. Therefore in the satellite-based melt-off retrieval the pixel is labelled "unclassified" if the number of observed (clear-sky) snow days is < 10% of the total number of days between the first observed snow day and the identified melt-off day. The pixel remains non-classified also in cases for which less than four snow days are identified for the whole season. Fig. 5 presents 0.1° melt-off day map (MoD_{Opt}) day for year 2007. In 2007 only sporadic snow days were present in Central Europe and thus most of the area remains unclassified.

3.3. Validation of melt-off day

To investigate the potential of CryoLand FSC maps and the melt-off detection algorithms described above in the European scale melt-off day mapping, we first carried out validation for the CryoLand-based melt-off day maps in the original 0.005° grid. The results are presented in Section 4.1. In order to make these estimates comparable with MoD_{MWR} and $TD_{FT\text{-}ESDR}$, the optical data based melt-off day maps were aggregated from 0.005° to 0.1° by averaging the obtained MoD-values within 20 × 20 pixel windows. If this window has > 20% of non-classified pixels, the 0.1° pixel is labelled non-classified as well. If a window has > 33% of water pixels, the 0.1° pixel is labelled "Water". The former threshold was derived from a statistical analysis on the typical MoD difference between spatially adjacent 0.005° pixels and the effect of this difference on the aggregated MoD. On average, five days of potential error is avoided when using the 20% threshold. The latter threshold was considered a compromise between ensuring that mixed land/water pixels are always land-dominated and at the same time, it does not overly reduce the classified area. The aggregation using the original melt-off day product instead of first aggregating the original FSC and then applying the MoD detection method was considered more reasonable. The latter approach would increase the FSC particularly near the areas where snow stays distinctively late, thus leading to unrealistic delay in the melt-off day in the coarser resolution pixel (in the worst case the permanent snow cover would hold the FSC above 0% throughout the year).

The validation of the melt-off day maps (MoD_{Opt}, MoD_{MWR}, $TD_{FT\text{-}ESDR}$) is carried out by comparing the values in 0.1° grid with the corresponding station's first snow-free day identified in the in situ SD time series (see Section 3.1). All three in situ datasets introduced in Section 2.4 are employed. RMSE, bias and correlation coefficient *r* are calculated. We also use Cumulative Distribution Functions (CDF) to visualize the results, as well as maps of the spatial distribution of error (estimated MoD − in situ MoD). These analyses are made for years 2001–2016, the period defined by the availability of Terra/MODIS and consequently, the CryoLand Pan-European FSC product. In addition we provide a short introduction to the performance of MoD_{MWR} and $TD_{FT\text{-}ESDR}$ for ~36 year time period 1980–2014 (2016 for MoD_{MWR}) separately for boreal forest and tundra areas.

3.4. Comparison of MoD_{Opt} and MoD_{MWR}

In addition to melt-off day detection made separately from optical and passive microwave data, a comparison of melt-off day derived from these two data sources is carried out. Again the analyses employ the datasets in 0.1° grid. The results identify where these two datasets are in agreement and where they are distinguishably different. This information serves the possible data fusion and choosing of the best possible dataset from a user's perspective. The maximum and minimum differences within the 16 year period are calculated. The results are presented as histograms with RMSE and bias provided. In addition, a map of differences is presented for pixels providing both MoD_{Opt} and MoD_{MWR}.

4. Results and discussion

4.1. Comparison of melt-off day retrieval from CryoLand FSC time series in 0.005° and 0.1° grids

The results for validation of MoD_{Opt} indicate that aggregating the FSC from 0.005° to 0.1° does not affect the obtained MoD significantly. The RMSE for 0.005° MoD is 12.84 days and for 0.01° MoD 13.12 days. The systematic error (bias, calculated as mean of differences) is slightly negative (−1.8 days) for 0.005° MoD, indicating that in general it tends to underestimate i.e. to provide too early estimates for melt-off day, although some cases indicate delayed melt identification. For 0.1° MoD, the bias is positive and only 0.9 days. Fig. 6a) depicts the behavior of MoD_{Opt} vs. MoD_{insitu} for both resolutions. The correlation coefficient is high for both resolutions. The results in Fig. 6a) indicate that the

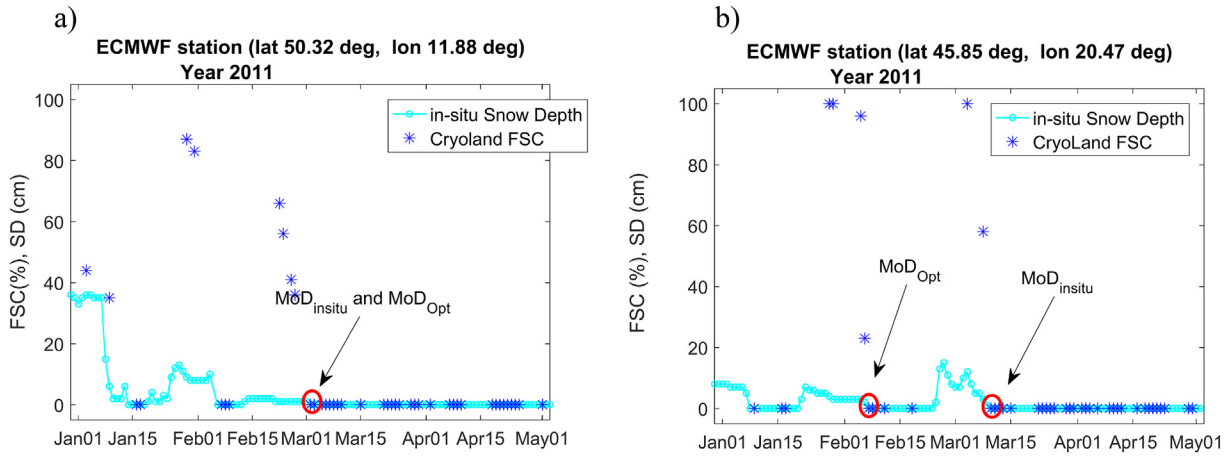

Fig. 7. Examples of a) a successful melt-off day identification with difference of 0 days and b) an unsuccessful identification showing underestimated melt-off day (difference is 31 days).

underestimations are associated to cases when snow melts quite early, around Day of Year 90 or less. Accuracy of the MoD estimates improves towards later in situ melt-off dates. Fig. 6b) presents the CDF for MoD differences in both resolutions; according to the CDF for MoD_{Opt} in 0.1° grid, the difference is < 10 days for 93% of all cases and more than −10 days for 8% of the cases. This implies that 85% of the differences are between −10 and 10 days. CDF for MoD_{Opt} in 0.005° grid is very similar. From these results we can deduce that aggregating from 0.005° to 0.01° does not affect the results significantly so we use the latter as a basis for further analyses. Thus, here onwards MoD_{Opt} refers to CryoLand FSC-based melt-off day maps in 0.1° grid.

The early MoD_{opt} MoDs are mainly caused by the lack of appropriate number of cloud-free FSC observations at the time of the actual MoD. This is typical for mid-latitudes (< 60°) with intermittent snow cover. When MoDs from both EO and in situ agree, there are cloud-free EO-data before and during the time of melt-off (Fig. 7a). However, our procedure for melt-off detection ignores EO snow observations if the melt-off has already been detected and there are only very few and sparse EO snow observations following it. In Fig. 7b) the first EO-based MoD takes place on 7th February which is quite correct according to the in situ observations, but after a few days a new snow period starts, followed by the final melt-off day on 10th March. But the two FSC observations just before the time of final (in situ-based) melt-off day are ignored since these observations might be due to a wrong snow commission, suspected to be snow/cloud confusion, and therefore are not reliable from the procedure's point-of-view. High-latitude areas with long seasonal snow cover are dominated by only small MoD differences, as the snow cover is continuous and is not characterized by intervening snow-free days which increase the probability of cloud-free EO-data at the crucial accumulating or melting events.

4.2. Validation of all three products related to snow clearance

Here we present the results for all three products for years 2001–2016, separately for all in situ sites and for combined boreal forest and tundra sites (as indicated by ESA GlobCover). The in situ melt-off day, derived as described in Section 3.1, is compared against MoD_{Opt} and MoD_{MWR} as well as against the freeze/thaw transition day by FT-ESDR, see Section 2.3. We combine the boreal forest and tundra sites in order to have an adequate number of cases to analyze. For the area of Europe, MoD_{Opt} (see Fig. 8a) has the best performance: RMSE = 13.12 days, bias = 0.9 days and r = 0.89 for all sites, while for boreal forest and tundra the values are 5.97, 1.26 and 0.92, correspondingly.

MoD_{MWR} (Fig. 8b) does not correspond to in situ melt-off day as well as MoD_{Opt}. For all in situ sites, the RMSE is significantly higher (29.14 days) than for MoD_{Opt}, however the bias is only slightly larger, −1.83 days, and r = 0.68. It should be noted here that these results were expected as the method by Takala et al. (2009) is designed for areas with continuous seasonal snow cover. This is realized when examining MoD_{MWR} for combined boreal forest and tundra: RMSE decreases to 14.03 days, with a slightly positive bias (2.05). r decreases to 0.58. It can be seen from Fig. 8b) that the decrease of r is due to two outliers (underestimations) present in the dataset. Their contribution to the correlation coefficient is strong due to the low amount of boreal forest and tundra sites (should these outliers be removed, r would increase to 0.78). The underestimations occur particularly when MoD_{insitu} < 100 days, thus supporting the fact MoD_{MWR} performs best in northern areas with a persistent snow season.

The results for $TD_{FT\text{-}ESDR}$ are presented in Fig. 8c). Despite the fact that the product does not directly describe the snow melt-off, it is well in accordance with in situ melt-off day, when all in situ sites are considered. RMSE = 26.29 days and bias = 3.94 days, r = 0.52. For the combined boreal forest and tundra sites, the RMSE = 15.85 days, bias = 1.70 days and r = 0.62. Fig. 8 indicates that for the in situ sites showing early melting, FT-ESDR provided a better estimate for melt-off day than the method by Takala et al. (2009). Since MoD_{MWR} and $TD_{FT\text{-}ESDR}$ both apply change detection to time-series of space-borne microwave radiometer observations, they have a strong correlation with each other and are therefore comparable. Finally, it is worth noting that although there may be deviation in the quality and representation of different in situ data sources (FMI, ECMWF, RIHMI), their density and spatial distribution in the northern and southern parts (as defined using latitude of 55° N) are rather similar, indicating that the differences in the validation results do not depend on the in situ data source but rather actually reflect the differences in snow conditions. A comparison of Earth observation-derived products against point-wise ground measurements is not straightforward, and the validation results are potentially affected by the uncertainty of the in situ observations and their spatial representativeness with respect to the grid size of the MoD-retrievals. In this paper, the uncertainty issue is neglected and in situ data are treated a “ground truth”.

Fig. 8d) presents the cumulative distribution for the difference (estimated MoD (or TD) − MoD_{insitu}) all the above six datasets (MoD_{Opt}, MoD_{MWR}, $TD_{FT\text{-}ESDR}$, all separately for all in situ sites and combined boreal forest and tundra sites). For MoD_{Opt} the deviation from MoD_{insitu} is roughly −10 to 10 days for ~85% of all in situ cases, while the same deviation for combined boreal forest and tundra sites is ~97%. For MoD_{MWR} the corresponding percentages are 52% and 82% (note the significant improvement in accuracy when only boreal forests and tundra are accounted for). For $TD_{FT\text{-}ESDR}$ the deviation from MoD_{insitu} is −10 to 10 days for 63% of all cases, and around the same (~63%) also

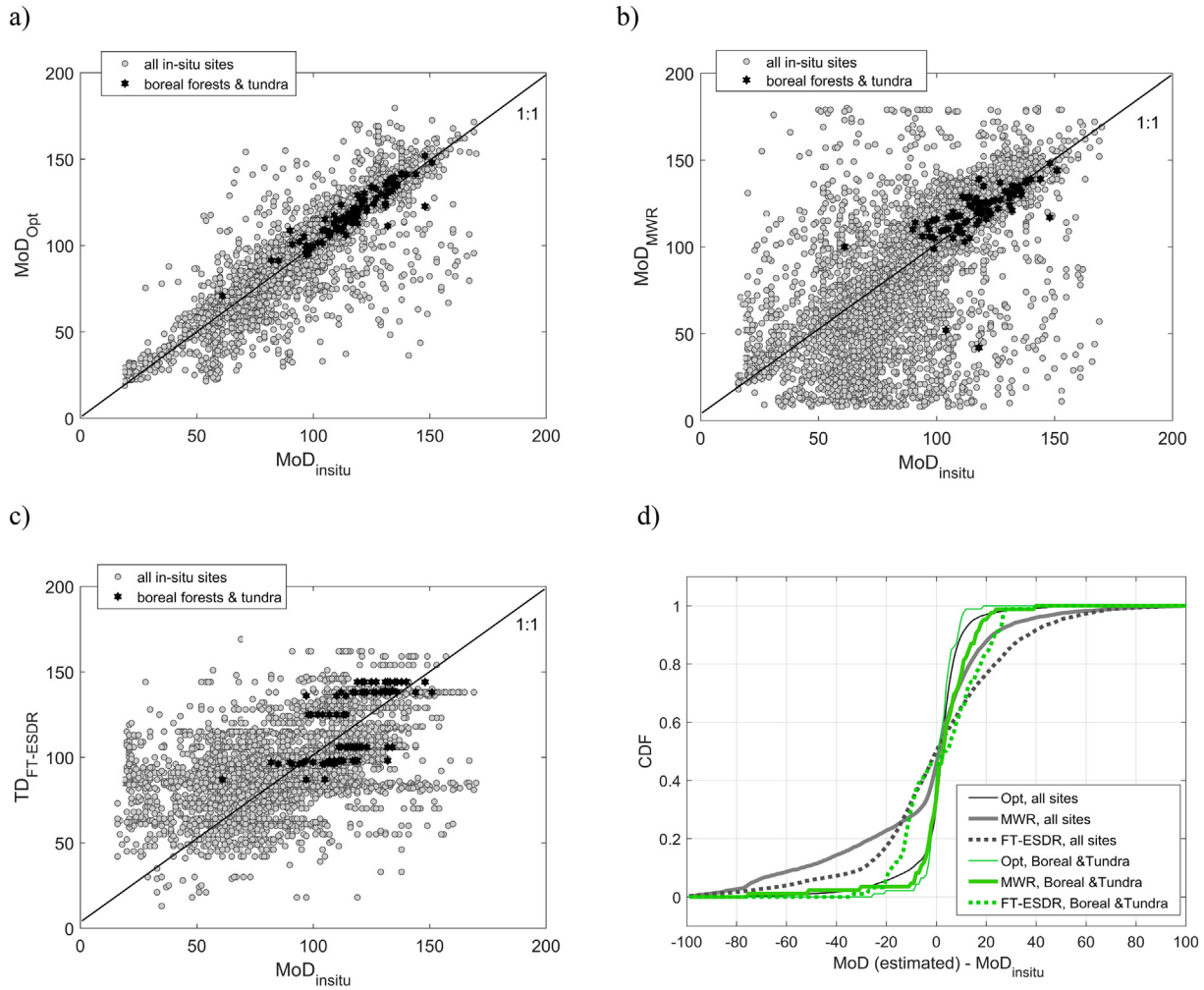

Fig. 8. Comparison of MoDs (TDs for FT-ESDR) against in situ MoD for years 2001–2016. a) MoD_{insitu} vs. MoD_{Opt}, b) MoD_{insitu} vs. MoD_{MWR}, c) MoD_{insitu} vs. $TD_{FT\text{-}ESDR}$, d) Cumulative Distribution Function for the differences (estimated MoD (TD) − MoD_{insitu}).

for boreal forest and tundra sites.

Fig. 9 presents the validation results for MoD_{MWR} and $TD_{FT\text{-}ESDR}$ in the original 25 km EASE-Grid, now calculated separately for tundra and boreal forests and for 37 years (35 for the FT-ESDR). Compared to the results shown above, the in situ network is sparser, since only synoptic weather stations from Finland, Russia, and Sweden are employed. Also, in this particular case the in situ MoD is produced applying a different protocol for identification of in situ melt-off day from SD time series, as explained in Section 3.1. Both comparisons are shown for European boreal forests and open high-latitude (tundra) areas within the Cryo-Land pan-European domain, see Fig. 1. The results indicate that for tundra and boreal forests MoD_{MWR} has a higher correlation with the in situ snow observed snow clearance than the FT-ESDR product: $r = 0.41$ for boreal forests and $r = 0.35$ for tundra, respectively. This was expected as FT-ESDR is actually a landscape freeze/thaw product, not specifically focused on snow melt. While the benefit of MoD_{MWR} is that

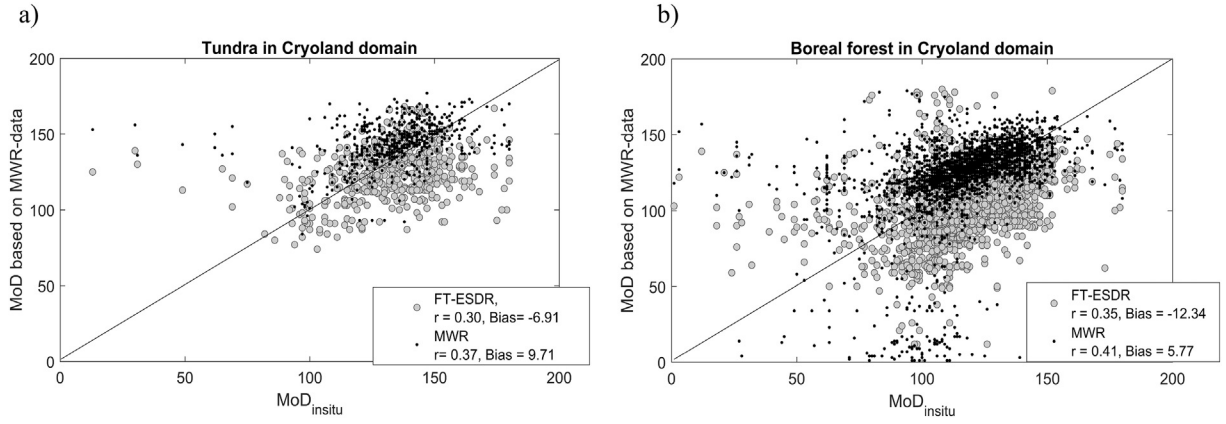

Fig. 9. MoD_{insitu} vs. MoD_{MWR} (years 1980–2016) and $TD_{FT\text{-}ESDR}$ (years 1980–2014) in 25 km EASE-Grid for a) tundra and b) boreal forests.

it is based solely on space-borne observations, it is well-suited only for high latitudes including boreal forest and tundra zones, and cold continental areas, i.e. regions with persistent, continuous seasonal snow cover (Fig. 8).

The locations of applied weather stations are mainly in Scandinavia and Finland with ephemeral/maritime to continental snow conditions (Fig. 3), depending on year and site. MoD_{MWR} is not able to properly capture snow conditions in some occasions, even though in general it performs well compared to $TD_{FT\text{-}ESDR}$. This is evident from Fig. 9) for the data points for which the estimated melt-off (MoD_{MWR}) occurs before the day 50, i.e. during January or February. Otherwise for MoD_{MWR} there is a positive bias (estimated − in situ) in comparisons with melt-off; the overestimations are caused by the point-wise nature of observations at synoptic stations that typically precede the snow clearance of a landscape (here regions with a nominal radiometer data processing size of 625 km^2). In some cases the synoptic station data indicated snow melt-off value is also apparently suspicious. In case of $TD_{FT\text{-}ESDR}$ the bias is negative, which is logical as the product indicates landscape thaw (including vegetation) that apparently precedes snow melt-off. All in all, there is an offset between MoD_{MWR} and $TD_{FT\text{-}ESDR}$ (Fig. 9), which originates from the different physical phenomena these two products are responding to.

4.3. The spatial distribution of estimated melt-off days vs. in situ observations

To better comprehend the spatial distribution of the accuracy of the estimated melt-off day, we prepared maps showing in situ site-specific differences (estimated MoD − MoD_{insitu}). Minimum and maximum of the average (over 16 years) site-specific differences are presented. Reddish colors (negative difference) indicate underestimated i.e. early MoD while bluish colors (positive difference) indicate overestimated i.e. too late MoD. Fig. 10 presents the minimum and maximum of the averaged differences calculated from data over melting seasons 2001–2016. For MoD_{Opt}, see in Fig. 10a and b, the clear distinction between mid- and high latitudes (> 60°) was expected, as the intermittent snow is easily omitted by optical data due to cloudiness, leading to underestimated of melt-off day (see red dots representing relatively strong underestimations in Central Europe, Fig. 10b). The overestimates are not as pronounced (see the light blue dots in Fig. 10a). For MoD_{MWR}, see Fig. 10c and d, the deviation is much higher, but the spatial distribution of the deviations is in agreement with MoD_{Opt}, except for mountain areas where there is a noticeable difference between MoD_{Opt} and MoD_{MWR}. Indeed it is worth noting that the accuracy of MoD_{MWR} for mountain areas (here the Alps) distinguishes from that of the plains remarkably, as MoD_{MWR} for mountains shows strong overestimations even in mid-latitudes. This feature probably is a consequence of the large footprint of the applied microwave radiometer measurements, which makes is difficult to capture the high spatial variation (driven by elevation gradients) in the timing of melt-off. A part of the stations in Fig. 10 are boreal forest and tundra stations, as indicated in Fig. 3.

4.4. The derived MoD (TD) trend for years 1980–2014 (2016)

Since the applied optical dataset is limited by the availability of Terra/MODIS acquisitions, most of our analyses are focused on the 2001–2016 time period. We derive a trend for melt-off day from the MWR-based datasets for the 35 year time period and compare it to the shorter trend obtained by MoD_{Opt}. The difference between trends provides valuable information for the future application of the data for the assessment of climate or phenological models. Fig. 11 presents the trend

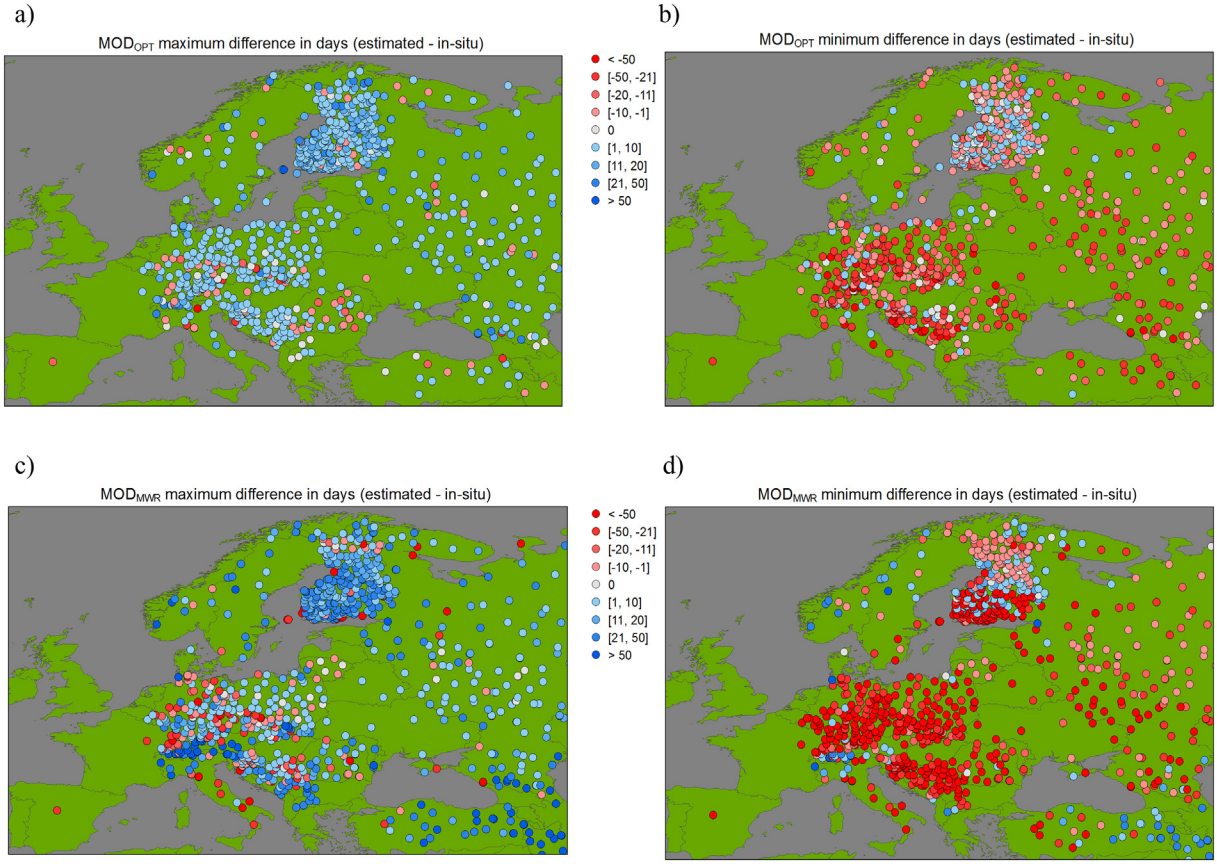

Fig. 10. The spatial distribution of the general (averaged over 16 years) deviation of the estimated MoD from the in situ MoD. a) Maximum difference for MoD_{Opt}, b) minimum difference for MoD_{Opt}, c) maximum difference for MoD_{MWR}, d) minimum difference for MoD_{MWR}.

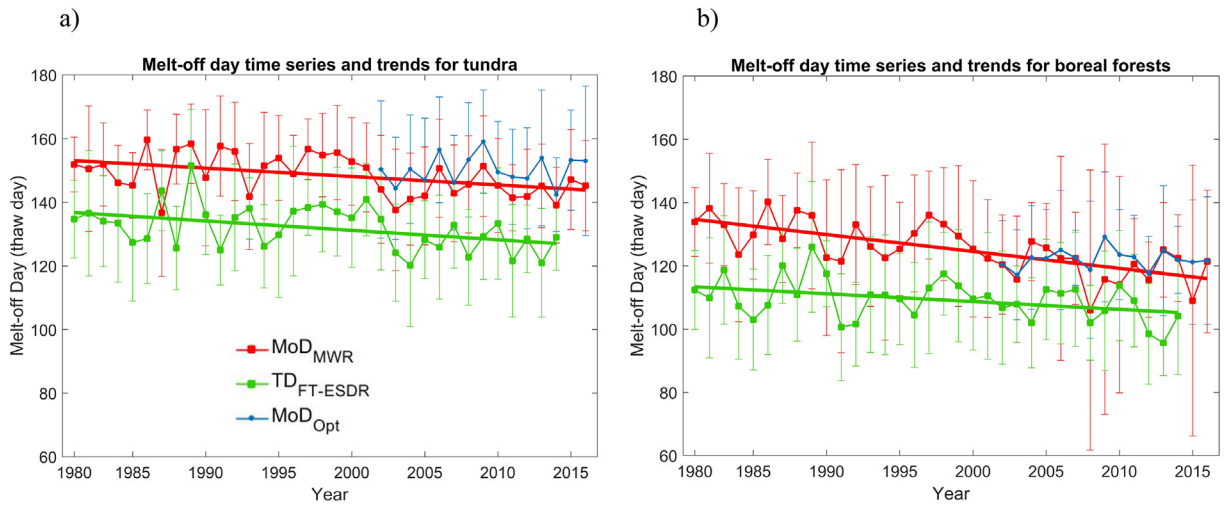

Fig. 11. The yearly means and trend of melt-off day (Thaw Day for FT-ESDR) for a) tundra and b) boreal forest sites (shown in Fig. 3). Vertical lines indicate the mean MoD ± standard deviation.

of MoD for a) tundra and b) boreal forests within Pan-European domain (see Fig. 4). Although $TD_{FT\text{-}ESDR}$ is systematically lower than MoD_{Opt} and MoD_{MWR} (since it does not measure the same phenomenon exactly), both microwave-data based datasets produce a similar decreasing trend. For tundra, both datasets show a decrease of ~3 days per decade. For boreal forest the trend from MoD_{MWR} shows a stronger decrease of ~5 days per decade, while $TD_{FT\text{-}ESDR}$ shows a decrease of only ~3 days per decade, just like for tundra. MoD_{Opt} agrees more closely with $MoD_{MWR,}$ which was expected due to the results discussed earlier in this paper.

4.5. Comparison of MoD_{Opt} and MoD_{MWR}

Here we provide statistics for differences $MoD_{Opt} - MoD_{MWR}$, i.e. relying only on EO-data. Fig. 12a presents the distribution of differences, as well as the RMSE and bias. The results indicate that MoD_{MWR} is typically later than MoD_{Opt} (bias = 9.6 days). However, the opposite is also possible since the RMSE is 25.32 days. It should be noted that the coverage of the analysis area is controlled by the availability of MoD_{Opt}. As it is already known from the results presented above that MoD_{MWR} has problems in areas with intermittent snow, we repeated the analysis for boreal forests and tundra, separately, see Fig. 12b and c. The results show a substantial decrease in RMSE and bias in boreal forests in particular, those being 16.7 and 1.9 days, respectively. For tundra area, the decrease is less pronounced. The probable reason for this is that tundra areas within our study domain comprise mostly mountains, that is, the ones remaining after exclusion of the steepest one as described in Section 2.4, where the footprint of the applied microwave radiometer is too large to capture the high spatial variation in timing of melt-off.

To identify the areas where these two datasets differ most, we calculated maps for the minimum and maximum differences ($MoD_{Opt} - MoD_{MWR}$), see Fig. 13. First, the difference was calculated for each pixel for each year; the final minimum and maximum for a pixel are the lowest and highest difference amongst the yearly differences, correspondingly. From the maximum difference it is evident that differences are highest at mid-latitudes (excluding the eastern parts of the area where snow cover period is typically long and continuous) and also in Southern Finland and Sweden. All these are areas with typically short and discontinuous snow cover. MoD_{MWR} may be as much as 80 days too early compared to MoD_{Opt}. At high-latitudes (practically in the boreal forest zone) the typical maximum difference is ~10 days. From the minimum differences we also see that for most of the non-mountainous Europe there are very rare cases when MoD_{MWR} takes place later than MoD_{Opt}. Thus, when there are remarkable differences these are predominantly due to too early MoD_{MWR}. The reason for this is that the snow melt algorithm by Takala et al. (2009) uses a relative difference of ΔTb to determine the snow melt-off. In practice the algorithm always generates an estimate of the melt-off even though the conditions for applying radiometer data are not optimal. In addition to the mixed pixel problem a shallow or very wet snowpack can cause problems since in either case the radiometer signature is weak.

5. Summary and conclusions

This paper describes the methodology for deriving yearly pixel-wise melt-off day maps from optical data-based FSC (Fractional Snow Cover) without conducting any interpolation for cloud-obscured pixels or otherwise missing data. The Copernicus CryoLand Pan-European FSC time series for 2001–2016 re-gridded to 0.1° served as input for production of 16 years' melt-off day maps (MoD_{Opt}) for Europe. These maps were compared with melt-off day maps produced with the passive microwave radiometer based method by Takala et al. (2009) (MoD_{MWR}), in order to gain a better understanding of the performance of these two independent datasets, particularly concerning the effect of geographical location and typical snow conditions on the accuracy of the melt-off day estimates. Both these datasets were also evaluated against melt-off day derived from in situ snow depth (SD) time series observed at European weather stations. We also investigated the relationship of these melt-off day products to the passive microwave radiometer-based freeze/thaw product of Earth System Data Record (FT-ESDR, here also re-gridded to 0.1°, denoted as $TD_{FT\text{-}ESDR}$; Kim et al. 2014). The time period of 2001–2016 was selected due to the availability of CryoLand FSC products relying on MODIS measurements. Our results clearly show that the melt-off day derived from optical springtime FSC time series provides the best correlation with the snow melt-off day as indicated by the weather station snow depth. The MoD_{Opt} bias to in situ observations varies by region with too early estimates at mid-latitudes and delayed estimates at high latitudes. Overall the deviation of MoD_{Opt} from MoD_{insitu} is quite small, with a positive bias of 0.9 days, while RMSE is 13.1 days. For 85% of the analyzed cases the difference between MoD_{Opt} and MoD_{insitu} are between −10 and 10 days. This accuracy is sufficient for instance in the modelling of animal phenology (Pöyry et al. 2017).

Melt-off day derived from MWR-based method by Takala et al. (2009) provides somewhat lower correlation with the snow clearance indicated by weather stations. Partly, the problem with MoD_{MWR} is the large footprint of the radiometer observation (25 km) which weakens the capability to detect local-scale variations in snow clearance timing,

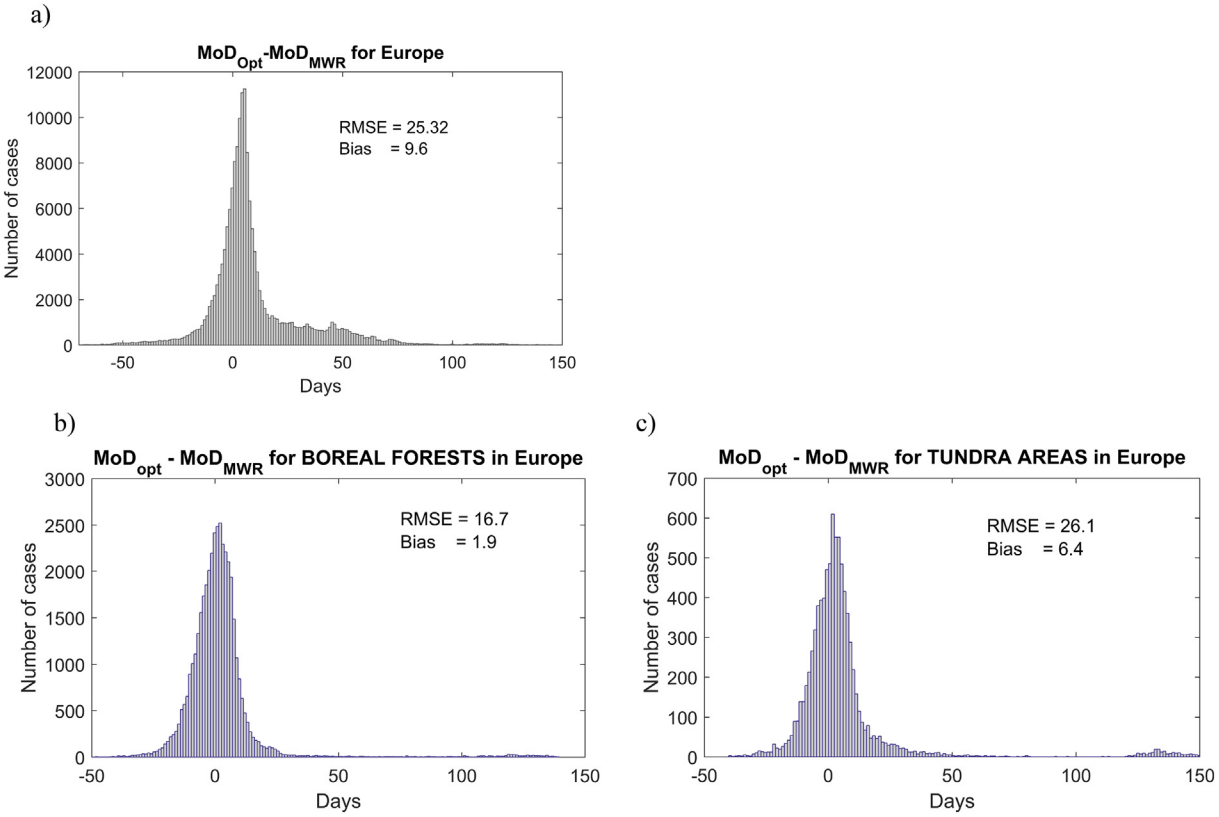

Fig. 12. Distribution and statistics for difference $MoD_{Opt} - MoD_{MWR}$ (years 2001–2016) for a) Europe, b) for European boreal forests and c) for European tundra.

controlled by heterogeneity in vegetation, aspect, etc. There are general limitations of microwave brightness temperature response to snow physical characteristics: the method cannot capture melt-off accurately for areas where snow has undergone several melt/freeze cycles. This is evident in our results showing a clearly more accurate timing of melt-off for regions with continuous seasonal snow than for regions with intermittent snow. For the whole Pan-European area the RMSE and bias for MoD_{MWR} are 29.1 and 1.8 days, respectively. Only 52% of the differences $MoD_{Opt} - MoD_{insitu}$ are between −10 and 10 days. However, it is seen from the generated maps of the spatial distribution of difference $MoD_{MWR} - MoD_{insitu}$, that the worst cases are concentrated in the mid-latitude with intermittent snow while much better accuracy is achieved for high-latitude areas. For boreal forest and tundra areas, the RMSE decreases to 14.0 days; also the percentage number given above (52% for all cases) increases substantially to 82%. These results evidently show that the method by Takala et al. (2009) provides reasonable accuracy i.e. useful information of melt-off day for areas with continuous seasonal snow cover, while we cannot recommend its use for areas of intermittent or ephemeral snow.

Since passive microwave radiometer observations date back several

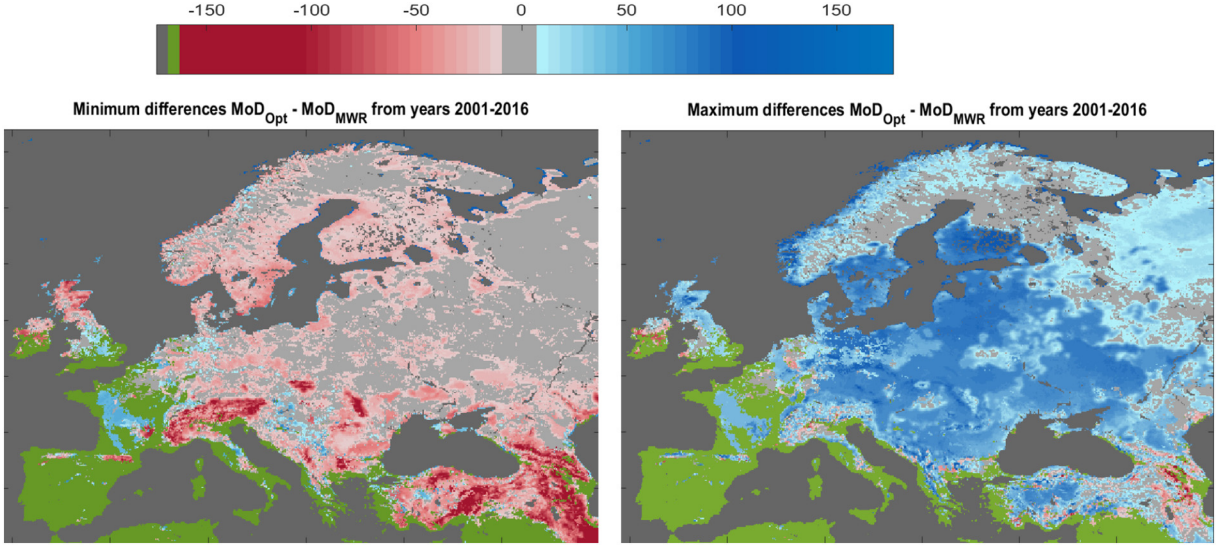

Fig. 13. Minimum and maximum melt-off day differences (in days) from melting seasons 2001–2016. Green color indicates the non-classified areas in MoD_{Opt}, dark grey represents water. (For interpretation of the references to color in this figure legend, the reader is referred to the web version of this article.)

decades, we also present an evaluation against in situ melt-off day for MoD_{MWR} and $TD_{FT\text{-}ESDR}$ for years 1980–2016 (1980–2014 for FT-ESDR; separately for tundra and boreal forests). Results indicate that snow melt day at European tundra sites shows a decrease of ~3 days per decade both by MoD_{MWR} and $TD_{FT\text{-}ESDR}$, while in boreal forests the trends are less similar; MoD_{MWR} shows a decreasing trend of 5 days per decade whereas $TD_{FT\text{-}ESDR}$ shows a decrease of 3 days per decade. This result (earlier melting over the long term) is in line with the results e.g. by Derksen and Brown (2012) and Mudryk et al. (2017), showing the reduction of snow-cover extent in the Northern Hemisphere and particularly in the Arctic. The FT-ESDR is well correlated with the MoD_{MWR} and MoD_{Opt}, but due to a different physical phenomenon it represents, there is an offset with the other two datasets. It is also noteworthy that overall, FT-ESDR provides better estimates for melt-off day (when compared to in situ) over the entire Europe, including areas of intermittent snow where MoD_{MWR} has difficulties.

Acknowledgements

This work was supported by the European Commission Framework Programme 7 via project CLIPC (Constructing Europe's Climate Information Portal) (grant no. 607418) and by the European Commission Life+ financial instrument via project Monimet (Grant agreement LIFE12 ENV/FI000409).The authors also thank EU Copernicus-programme for the possibility to generate the CryoLand dataset (through project CryoLand, 2011–2015, No. 262925).

References

Ackerman, S., Frey, R., Strabala, K., Liu, Y., Gumley, L., Baum, B., Menzel, P., 2010. Discriminating Clear-Sky from Cloud with MODIS — Algorithm Theoretical Basis Document. Products: 35_L2.

Aurela, M., Laurila, T., Tuovinen, J.-P., 2004. The timing of snow melt controls the annual CO_2 balance in a subarctic fen. Geophys. Res. Lett. 31, L16119. http://dx.doi.org/10.1029/2004GL020315.

Barlage, M., Zeng, X., Wei, H., Mitchell, K., 2005. A global 0.05° maximum albedo dataset of snow-covered land based on MODIS observations. Geophys. Res. Lett. 32 (17).

Bartholome, E.M., Belward, A.S., 2005. GLC2000; a new approach to global land cover mapping from Earth observation data. Int. J. Remote Sens. 26, 1959–1977.

Bontemps, S., Defourny, P., Van Bogaert, E., Arino, O., Kalogirou, V., Ramos Perez, J.J., 2009. GLOBCOVER 2009 Products Description and Validation Report, Université catholique de Louvain (UCL) & European Space Agency (ESA), Vers. 2.2. 53 pp, hdl:10013/epic.39884.d016, 2011.

Böttcher, K., Aurela, M., Kervinen, M., Markkanen, T., Mattila, O.-P., Kolari, P., Metsämäki, S., Aalto, T., Arslan, A.N., Pulliainen, J., 2014. MODIS time-series-derived indicators for the beginning of the growing season in boreal coniferous forest — a comparison with CO_2 flux measurements and phenological observations in Finland. Remote Sens. Environ. 140, 625–638.

Bulygina, O.N., Razuvaev, V.N., Aleksandrova, T.M., 2015. Description of Data Set "Routine Snow Surveys". http://meteo.ru/english/climate/descrip9.htm.

Choi, G., Robinson, D.A., Kang, S., 2010. Changing northern hemisphere snow seasons. J. Clim. 23, 5305–5310.

Cooper, E.J., Dullinger, S., Semenchuk, P., 2011. Late snowmelt delays plant development and results in lower reproductive success in the High Arctic. Plant Sci. 180, 157–167.

Derksen, C., Brown, R., 2012. Spring snow cover extent reductions in the 2008–2012 period exceeding climate model projections. Geophys. Res. Lett. 39, L19504. http://dx.doi.org/10.1029/2012GL053387.

Déry, S.J., Brown, R., 2007. Recent Northern Hemisphere snow cover extent trends and implications for the snow-albedo feedback. Geophys. Res. Lett. 34, L22504.

Dietz, A.J., Wohner, C., Kuenzer, C., 2012. European snow cover characteristics between 2000 and 2011 derived from improved MODIS daily snow cover products. Remote Sens. 4, 2432–2454. http://dx.doi.org/10.3390/rs4082432.

Grippa, M., Kergoat, L., Le Toan, T., Mognard, N.M., Delbart, N., L'Hermitte, J., Vicente-Serrano, S.M., 2005. The impact of snow depth and snowmelt on the vegetation variability over central Siberia. Geophys. Res. Lett. 32.

Hall, D.K., Riggs, G.A., Salomonson, V.V., 1995. Development of methods for mapping global snow cover using moderate resolution imaging spectroradiometer data. Remote. Sens. Environ. 54, 127–140.

Kim, Y., Kimball, J.S., McDonald, K.C., Glassy, J., 2011. Developing a global data record of daily landscape freeze/thaw status using satellite passive microwave remote sensing. IEEE Trans. Geosci. Remote Sens. 49, 949–960.

Kim, et al., 2014. MEaSUREs Global Record of Dailyl Landscape Freeze/Thaw Status, Version 3. NASA National Snow and Ice Data Center Distributed Active Archive Center, Boulder, Colorado, USA. http://dx.doi.org/10.5067/MEASURES/CRYOSPHERE/nsidc-0477.003.

Kitaev, L., Kislov, A., Krenke, A., Razuvaev, V., Martuganov, R., Konstantinov, I., 2002. The snow characteristics of northern Eurasia and their relationship to climatic parameters. Boreal Environ. Res. 7, 437–445.

Lindsay, Chuck, et al., 2015. Deriving snow cover metrics for Alaska from MODIS. Remote Sens. 7 (10), 12961–12985. http://dx.doi.org/10.3390/rs71012961.

Metsämäki, S., Anttila, S., Huttunen, M., Vepsäläinen, J., 2005. A feasible method for fractional snow cover mapping in boreal zone based on a reflectance model. Remote Sens. Environ. 95 (1), 77–95.

Metsämäki, S., Mattila, O.-P., Pulliainen, J., Niemi, K., Luojus, K., Böttcher, K., 2012. An optical reflectance model-based method for fractional snow cover mapping applicable to continental scale. Remote Sens. Environ. 123, 508–521.

Metsämäki, S., Pulliainen, J., Salminen, M., Luojus, K., Wiesmann, A., Solberg, R., Böttcher, K., Hiltunen, M., Ripper, E., 2015. Introduction to Globsnow Snow Extent products with considerations for accuracy assessment. Remote Sens. Environ. 156 (2015), 96–108.

Mudryk, L., Kushner, P., Derksen, C., Thackeray, C., 2017. Snow cover response to temperature in observational and climate model ensembles. Geophys. Res. Lett. 44. http://dx.doi.org/10.1002/2016GL071789.

Nagler, T., Bippus, G., Schiller, C., Metsämäki, S., Mattila, O.-P., Luojus, K., Malnes, E., Solberg, R., Diamandi, A., Larsen, H.E., Wiesmann, A., Gustafsson, D., 2015. CryoLand — Copernicus Service Snow and Land Ice: Final Report. pp. 46. available at. http://cryoland.eu. http://enveo.at.

Pöyry, J., Böttcher, K., Fronzek, S., Gobron, N., Leinonen, R., Metsämäki, S., Virkkala, R., 2017. Predictive power of remote sensing vs. temperature-derived variables in modelling phenology of herbivorous insects. Remote Sens. Ecol. Conserv. http://dx.doi.org/10.1002/rse2.56.

Qu, X., Hall, A., 2007. What controls the strength of snow-albedo feedback? J. Clim. 20, 3971–3981. http://dx.doi.org/10.1175/JCLI4186.1.

Räisänen, P., Luomaranta, A., Järvinen, H., Takala, M., Jylhä, K., Bulygina, O.N., Luojus, K., Riihelä, A., Laaksonen, A., Koskinen, J., Pulliainen, J., 2014. Evaluation of North Eurasian snow-off dates in the ECHAM5.4 atmospheric general circulation model. Geosci. Model Dev. 7, 3037–3057. http://dx.doi.org/10.5194/gmd-7-3037-2014.

Schwaizer, G., Ripper, E., Nagler, T., Ikonen, J., Luojus, K., Ryyppö, T., Hiltunen, M., Pulliainen, J., Metsämäki, S., 2017. Upgraded Pan-European Snow Services. CryoLand Report ID4.6/A. pp. 31. available at. http://cryoland.eu.

Takala, M., Pulliainen, J., Metsämäki, S., Koskinen, J., 2009. Detection of snowmelt using spaceborne microwave radiometer data in Eurasia from 1979 to 2007. IEEE Trans. Geosci. Remote Sens. 47 (9).

Takala, M., Luojus, K., Pulliainen, J., Derksen, C., Lemmetyinen, J., Kärnä, J.-P., Koskinen, J., Bojkov, B., 2011. Estimating northern hemisphere snow water equivalent for climate research through assimilation of space-borne radiometer data and ground-based measurements. Remote Sens. Environ. 115 (12), 3517–3529. ISSN 0034-4257. https://doi.org/10.1016/j.rse.2011.08.014.

Thackeray, C.W., Fletcher, C.G., Derksen, C., 2014. The influence of canopy snow parameterizations on snow albedo feedback in boreal forest regions. J. Geophys. Res. Atmos. 119, 9810–9821. http://dx.doi.org/10.1002/2014JD021858.

Thum, T., Aalto, T., Laurila, T., Aurela, M., Hatakka, J., Lindroth, A., Vesala, T., 2009. Spring initiation and autumn cessation of boreal coniferous forest CO_2 exchange assessed by meteorological and biological variables. Tellus B 61, 701–717.

Vaganov, E.A., Hughes, M.K., Kirdyanov, A.V., Schweingruber, F.H., Silkin, P.P., 1999. Influence of snowfall and melt timing on tree growth in subarctic Eurasia. Nature 400, 149–151.